

# Ring-Opening Polymerization of Epoxides Catalyzed by Uranyl Complexes: An Experimental and Theoretical Study of the Reaction Mechanism

Jian Fang,<sup>†,‡</sup> Aurora Walshe,<sup>§</sup> Laurent Maron,<sup>\*,‡</sup> and Robert J. Baker<sup>\*,§</sup>

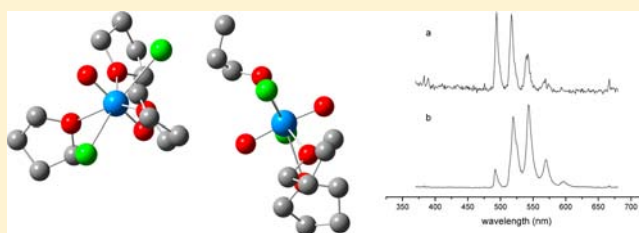
<sup>†</sup>College of Chemistry and Chemical Engineering, Lanzhou University, Lanzhou 730000, China

<sup>‡</sup>LPCNO, INSA Toulouse, 137 Avenue de Rangueil, 31077 Toulouse, France

<sup>§</sup>School of Chemistry, University of Dublin, Trinity College, Dublin 2, Ireland

## Supporting Information

**ABSTRACT:** A comprehensive computational study on the ring-opening polymerization of propylene oxide catalyzed by uranyl chloride  $[\text{UO}_2\text{Cl}_2(\text{THF})_3]$  and the uranyl aryloxy  $[\text{UO}_2(\text{OAr})_2(\text{THF})_2]$  ( $\text{Ar} = 2,6\text{-}^t\text{Bu}_2\text{C}_6\text{H}_3$ ) is reported. The initiation and propagation steps have been probed and significant differences between the two catalysts discovered. The initiation step involving uranyl chloride is an intermolecular process because the orientation of the lone pair on the initiating chloride nucleophile is optimally oriented toward the empty  $\sigma^*$ -antibonding orbital of the epoxide, which lowers the activation barrier by 22 kcal mol<sup>-1</sup>. Thus, initiation is orbitally controlled. Propagation occurs through a dimeric species, and low-temperature fluorescence spectroscopy has been used to probe this experimentally. In contrast the initiation step for the uranyl aryloxy catalyzed mechanism is intramolecular because of the steric constraints imposed by the bulky substituents on the aryl ring and the fact that the lone pair on the nucleophile is able to approach the propylene oxide coordinated to the same uranium center. Thus, initiation is principally sterically controlled. Propagation is, however, intermolecular, and this can be traced to steric effects. Experimental evidence in the form of fluorescence spectroscopy and diffusion NMR has been used to explore the propagation process in solution.



## INTRODUCTION

The coordination and organometallic chemistry of uranium has undergone a renaissance of interest over the past few years.<sup>1</sup> Studies have identified unique transformations that have no parallel using d-block metal complexes, most impressively in small-molecule activation by uranium(III) compounds.<sup>2</sup> Catalytic applications are almost exclusively centered on uranium and thorium in their 4+ oxidation state, with  $[\text{Cp}^*_2\text{AnMe}_2]$  (**I**) and its derivatives (**II–IV**) the most comprehensively explored.<sup>3</sup> However, recently other compounds have begun to be examined as catalysts, such as the ferrocenylamide-supported uranium alkyl complex **V**<sup>4</sup> and the simple cationic species **VI** (Chart 1).

The classes of reactions catalyzed are now rather impressive and include polymerization of alkenes, dimerization and oligomerization of alkynes, hydrosilylation of alkenes and alkynes, and inter- and intramolecular hydroamination and hydrothiolation of alkenes and alkynes. Oxygen-containing monomers have been far less studied because conventional wisdom indicates that the hard oxophilic metal center will either simply coordinate the monomer with no further elaboration or prove susceptible to product inhibition. An example of this was contained in an early report by Lin and Marks, who demonstrated a marked decrease in the rate of hydrogenolysis of the meta-bound alkyl group in  $[\text{Cp}^*_2\text{Th}$

(R)(OR)] relative to that in  $[\text{Cp}^*_2\text{ThR}_2]$ .<sup>5</sup> Quite recently, however, this myth has been challenged by Eisen and co-workers in studies on the ring-opening polymerization of  $\epsilon$ -caprolactone.<sup>6</sup> In addition, a Tishchenko reaction<sup>7</sup> using the metallocene-based catalyst **I** and the cationic **V** has been reported. Notably, however, the use of higher-oxidation-state organometallic uranium compounds in catalysis is limited to the  $[\text{Cp}^*_2\text{U}(=\text{NAd})_2]$ -mediated reduction of azides.<sup>8</sup> There are very few examples of the uranyl ( $\text{UO}_2^{2+}$ ) moiety acting as a catalyst.<sup>9</sup> We recently demonstrated that epoxides are suitable substrates for ring-opening polymerization catalyzed by the simple coordination compound uranyl chloride (**1**) or a uranyl aryloxy,  $[\text{UO}_2(\text{OAr})_2(\text{THF})_2]$  ( $\text{Ar} = 2,6\text{-}^t\text{Bu}_2\text{C}_6\text{H}_3$ ) (**2**; Chart 2).<sup>10</sup> Our hypothesis for the choice of this ligand and metal combination in **2** was as follows: (a) Because of the participation of *f* orbitals in bonding, the uranyl moiety is always trans, which leaves the remainder of the coordination chemistry to occur in the equatorial plane. Using suitably sterically encumbered ligands to control the equatorial coordination sphere, mutually cis ligand and solvent molecules can be coordinated. A catalytically competent geometry is an inherent property of the uranyl moiety, which is trivial to

Received: July 20, 2012

Published: August 6, 2012

Chart 1. Uranium(IV) Compounds Used as (Pre)catalysts

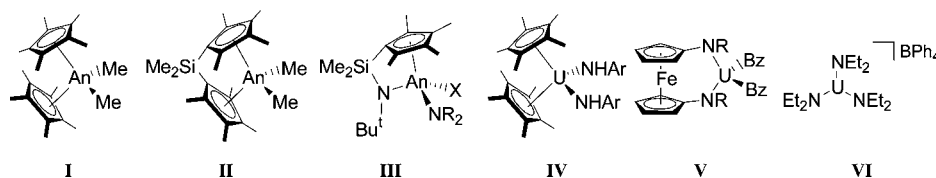
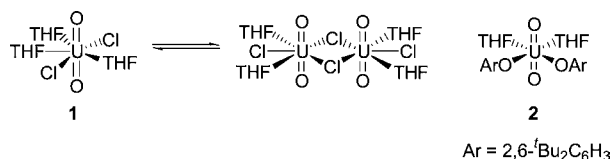


Chart 2. Uranyl Catalysts for the Ring-Opening Polymerization of PO



prepare. (b) A strong U–O bond<sup>11</sup> in the (pre)catalyst is replaced by a U–O bond in the propagating polymer so that the contribution from enthalpy will be small and the polymerization will be entropically controlled. (c) There is an additional energetic contribution from the release of ring strain of the three-membered ring.<sup>12</sup> (d) The nuclearity of actinide compounds is generally driven by the steric influence of the ligand, so discrete mononuclear uranyl aryloxides are readily prepared.<sup>13</sup>

The principle goal of this study is an in-depth exploration of the mechanism of the ring-opening polymerization of epoxides catalyzed by these uranyl compounds using computational methods. Compounds of the actinides present unique challenges for theoretical studies because relativistic effects and electron correlation effects of generally open-shell multiconfigurational compounds require careful analysis.<sup>14</sup> Notwithstanding these challenges, theoretical chemistry has been used extensively to explore some of the unique reactivity that experimental studies have reported and where *in silico* chemistry is substantially easier than experimental studies, for example, on *trans*-uranic compounds.<sup>15</sup> It is noteworthy that the calculations presented herein represent some of the largest to date (especially for mechanistic studies where the transition states (TSs) have been located) and demonstrate that computational actinide chemistry is developing to the same level of sophistication as that associated with transition-metal compounds, which are almost considered routine. In order to support the computational results, further experimental evidence for the mechanism will also be presented.

## EXPERIMENTAL SECTION

All manipulations were carried out using standard Schlenk and glovebox techniques under an atmosphere of high-purity argon. Spectroscopic-grade tetrahydrofuran (THF) was distilled over potassium. <sup>1</sup>H NMR spectra were recorded on a Bruker AV400 spectrometer operating at 400.13 MHz and referenced to the residual <sup>1</sup>H resonances of the solvent used. Details of the diffusion NMR can

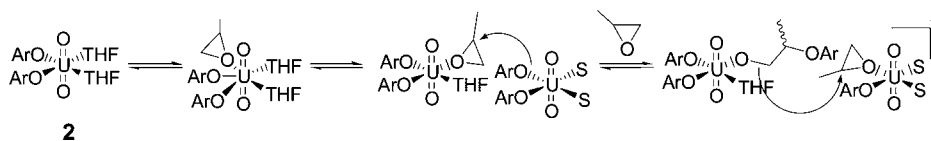
be found in the Supporting Information. UV–vis/near-IR spectra were obtained using a Perkin-Elmer Lambda 1050 spectrometer, and fluorescence spectra were measured on a Horiba-Jobin-Yvon Fluorolog-3 spectrometer. The complexes [UO<sub>2</sub>Cl<sub>2</sub>(THF)<sub>3</sub>]<sup>16</sup> and [UO<sub>2</sub>(OAr)<sub>2</sub>(THF)<sub>2</sub>]<sup>13</sup> were prepared by literature procedures, and all other reagents were obtained from commercial sources, dried over CaH<sub>2</sub>, and distilled under argon before use.

## COMPUTATIONAL DETAILS

In view of the good performance of density functional theory (DFT), we were prompted to perform DFT calculations at the B3PW91 level of theory on all stationary points of the potential energy surfaces that we studied using the *Gaussian09* program suite.<sup>17</sup> The equilibrium and transition structures were fully optimized at the Becke's three-parameter hybrid functional<sup>18</sup> combined with the nonlocal correlation functional provided by Perdew/Wang.<sup>19</sup> RECP (augmented by a *f* polarization function,  $\alpha = 1.0$ ) adapted to the oxidation state VI+ was used for the reactions.<sup>20</sup> The correctness of the latter is well documented in previous publications from our group.<sup>21</sup> For the rest of nonmetal atoms, the 6-31G(d,p) basis set was used.<sup>22</sup> In all computations, no constraints were imposed on the geometry. Full geometry optimization was performed for each structure using Schlegel's analytical gradient method,<sup>23</sup> and attainment of the energy minimum was verified by calculating the vibrational frequencies that result in the absence of imaginary eigenvalues. All stationary points have been identified for minimum (number of imaginary frequencies  $N_{\text{imag}} = 0$ ) or TSs ( $N_{\text{imag}} = 1$ ). The vibrational modes and corresponding frequencies are based on a harmonic force field. This was achieved with a self-consistent-field convergence on the density matrix of at least  $10^{-9}$  and a root-mean-square force of less than  $10^{-4}$  au. All bond lengths and angles were optimized to better than 0.001 Å and 0.1°, respectively. Gibbs free energies were obtained at  $T = 298.15$  K within the harmonic approximation. Intrinsic reaction paths (IRPs)<sup>24</sup> were traced from the various transition structures to ensure that no further intermediates exist.

## RESULTS AND DISCUSSION

In our previous experimental study on the ring-opening polymerization of epoxides catalyzed by **1** and **2**, we reported strong evidence for an intermolecular mechanism, with a back-side attack of the nucleophile at an epoxide coordinated to a second uranium center (Scheme 1).<sup>10</sup> Intriguingly, all epoxide polymerizations catalyzed by transition- and main-group-metal compounds that have been studied mechanistically follow this route.<sup>25</sup> A substantial body of evidence has been presented that concludes that this pathway is also followed in CO<sub>2</sub>/epoxide copolymerizations.<sup>26</sup> Moreover, there is a mechanistic similarity to the enantioselective ring opening of epoxides studied

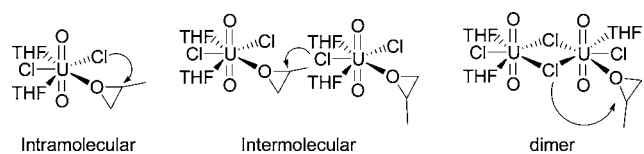
Scheme 1. Postulated Initiation and Propagation for Ring-Opening Polymerization of PO by the Uranyl Aryloxide Catalyst **2** (Ar = 2,6-tBu<sub>2</sub>C<sub>6</sub>H<sub>3</sub>)

extensively by Jacobsen<sup>27</sup> and more recently to the enantioselective ring-opening polymerization of (*R*)- or (*S*)-propylene oxide (PO) reported by Coates et al.<sup>28</sup>

To gain a deeper understanding of the mechanism of our uranyl-catalyzed reaction, we have undertaken a comprehensive computational study on both uranyl chloride, **1**, and uranyl aryloxide, **2**. In noncoordinating solvents, **1** exists as the dimer  $[\text{UO}_2\text{Cl}_2(\text{THF})_2]_2$ , so the reaction mechanism involving this species was also considered, although upon the addition of epoxide, we postulated that the monomeric species  $[\text{UO}_2\text{Cl}_2(\text{THF})_x(\text{epoxide})_y]$  was preferentially formed. For the sake of clarity, the uranyl chloride and uranyl aryloxide catalysts will be discussed separately.

**Catalysis by Uranyl Chloride (1).** Three different reaction pathways have been computed, namely, intra- and intermolecular ring opening and one involving a dimeric species (Scheme 2). On the basis of a spectroscopic study of the

**Scheme 2. Three Pathways Computed for the First Ring-Opening Step of PO Catalyzed by Uranyl Chloride**



polymer microstructure, the intermolecular mechanism was proposed experimentally.<sup>10</sup> The two first insertions were considered for PO, and in all cases, the ring opening on the two different carbon centers has been computed. Because of the well-known problem of correctly computing the entropy (especially when several insertion steps and molecules are computed), the profiles are reported in enthalpy at 298.15 K (Figure 1). The computed effect of including solvent by means

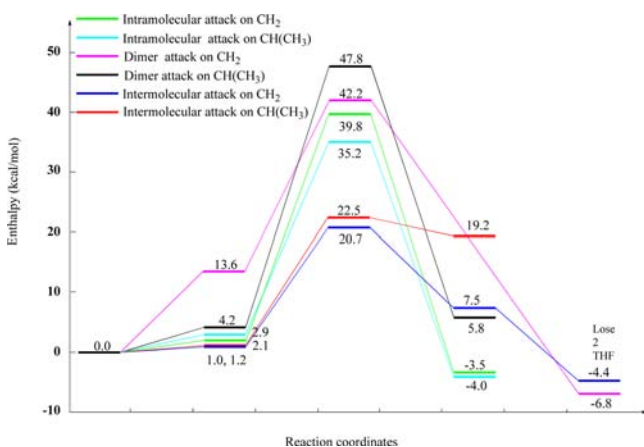


**Figure 1.** Enthalpy energy profile at 298.15 K for the first step of the reaction of PO with  $[\text{UO}_2\text{Cl}_2(\text{THF})_3]$ .

of full geometry optimization within the conductor-like polarizable continuum model (CPCM) was found to be small on the enthalpy (less than 1 kcal·mol<sup>-1</sup>) and has not been considered in the following. It should be noticed that standard single-point calculations in CPCM on the gas-phase geometry would predict changes of up to 20 kcal·mol<sup>-1</sup>, so that one has to properly account for solvent effects.

In all computed cases, the replacement of a coordinated THF molecule by a PO is computed to be favorable, at around 1

kcal·mol<sup>-1</sup> in the best cases. Because of the ring strain in the epoxide, the oxygen lone pair is in an orbital of increased *s* character, which would make the PO less basic than THF.<sup>29</sup> Therefore, for this step to be favorable, binding to the hard metal ion must be accompanied by polarization of the C–O bond and quasi-carbocationic character. This is confirmed by inspection of the C–O bond lengths in the three-membered ring, which are 1.456 and 1.444 Å (cf. 1.427 and 1.425 Å in free PO). The U–O bond length is 2.460 Å, and the U=O bond length is 1.735 Å. For comparison, in **1**, the U–O bonds of the coordinated THF are 2.443(6), 2.464(5), and 2.467(6) Å, while the U=O bond length is 1.766(6) Å.<sup>16</sup> The uranyl U=O bond length is known to be somewhat sensitive to the electronic environment,<sup>30</sup> and this metrical parameter indicates that the electronic environment around the uranium center is barely perturbed upon ligand exchange.

From the adduct, the system has to reach the nucleophilic attack (NA) TS. At this stage, important differences are observed between the three sets of catalysts that were considered. The highest barrier (more than 40.0 kcal·mol<sup>-1</sup>) is found for the dimer, indicating that the polymerization reaction cannot occur at this species. This is due to the fact that the U...U distance is controlled in the dimer by the bridging chlorine atom. Thus, the stabilizing presence of the bridge induces a steric constraint that destabilizes the TS (Figure 2a).

The intramolecular pathway leads to barriers around 35.0 and 40.0 kcal·mol<sup>-1</sup>. This result is in excellent agreement with the experimental study, which showed that chloride ligands are not as efficient initiator ligands for ring-opening polymerization compared to uranyl aryloxide (vide infra). This is due to the strong directionality of the chloride orbitals that has to be enforced to point toward the empty  $\sigma^*$  orbital on the PO, which is along the C–O bond axis. Indeed, coordination to only one metal center does not allow an easy process (Figure 2b) and is consistent with Baldwin's rules for an endo-trig-type cyclization (while only being strictly valid for first-row transition metals; Scheme 3). On the other hand, removing the constraint by involving a second metal center clearly improved the results. Indeed, when the activated PO is coordinated to one uranium center and the chloride is coordinated to another uranium center, this allows an optimal orientation of its lone pair toward the empty C–O  $\sigma^*$  orbital of the PO due to the lack of constraint of the rigid structure of the dimer. This leads to a substantial lowering of the activation barrier (around 21.0–22.0 kcal·mol<sup>-1</sup>), indicating that this is the kinetically favored pathway.

On this basis, only the geometry of the intramolecular TS will be discussed in the following. At the TS (Figure 2c), the ring is already opened (C–O distances of 2.0248 and 1.394 Å), but neither the C–Cl nor the U–O bonds are already fully formed (2.346 and 2.223 Å). The TS is thus strongly ionic in character, as further substantiated by the natural bond order analysis (APT charges: C, 1.1809; O, -1.4090). This is also in line with the computed slight kinetic preference for the NA to take place at the prochiral center (secondary carbon) than at the primary carbon of the PO molecule (although the difference is within the error bar of the method). This preference was also reported experimentally, although some regioirregular insertions were noted in the polymer. As expected, attack at the prochiral center induces a better stabilization of the carbocation at the TS, allowing a facile attack of the chloride. From a thermodynamic point of view, the reaction is predicted to be endergonic by 7.5 kcal·mol<sup>-1</sup>

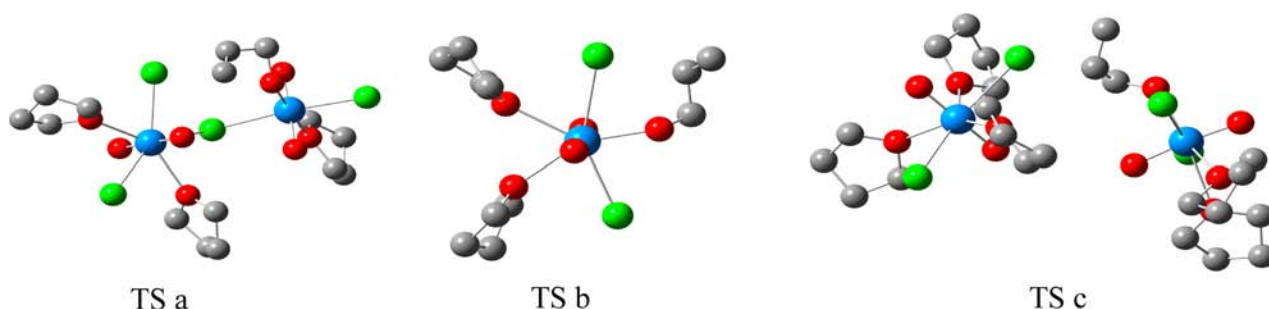
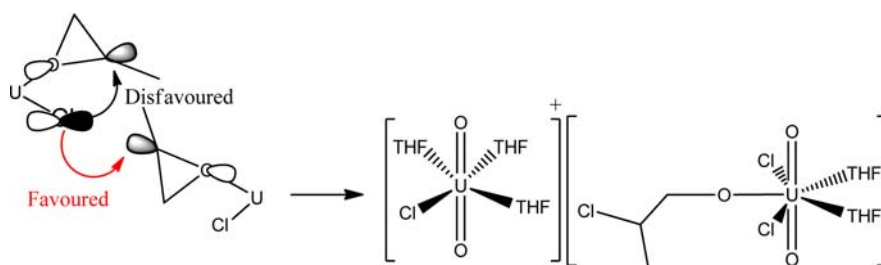


**Figure 2.** 3D representations of the three TSs computed for uranyl chloride: TS a is for a dimeric mechanism; TS b is for an intramolecular mechanism; TS c is for an intermolecular mechanism.

### Scheme 3. Schematic Representation of the Intra- and Intermolecular Pathways



because of the lack of stabilizing orbital interaction of the formed ion pair  $[\text{UO}_2\text{Cl}(\text{THF})_2]^+[\text{UO}_2\text{Cl}_2(\text{OCH}_2\text{CCHMe})(\text{THF})]^-$ . However, this ion pair can undergo an isomerization process to form a weakly bonded dimer with a bridging chloride concomitant with the loss of a second THF molecule. This is reminiscent of a cation–cation interaction, with a desymmetrization of the  $\text{U}=\text{O}$  bond lengths ( $\text{U}=\text{O} = 1.75$  and  $1.83$  Å) and a  $\text{U}\cdots\text{O}(=\text{U})$  distance of  $2.387$  Å. For cation–cation interactions, the  $\text{U}=\text{O}$  bond is typically elongated to ca.  $1.82$  Å.<sup>31</sup> It is noteworthy that this isomerization was observed during the course of the geometry optimization of the product (from IRC) and no double-bridging chloride dimer was found (it may exist but was not observed during this optimization). The stabilization due to this isomerization is computed to be  $11.9$  kcal·mol<sup>-1</sup>, leading to an overall exergonic reaction.

These results show that coordination of the epoxide is not significantly affected by the nature of the uranyl complex and is not rate-determining, something that was inferred experimentally and is consistent with <sup>113</sup>Cd NMR studies of epoxide coordination to  $[\text{TpCd}(\text{OAc})]$  [Tp = hydrotris(3-phenylpyrazol-1-yl)borate],<sup>32</sup>  $[(\text{ArO})_2\text{Cd}(\text{solv})_{2-3}]$  (Ar = 2,6- $\text{R}_2\text{C}_6\text{H}_3$ ; R = Ph, <sup>t</sup>Bu, Me; Solv = THF, THT, pyridine, propylene carbonate),<sup>33</sup> and the unsolvated  $[(\text{ArO})_2\text{Cd}]_2$ .<sup>34</sup> The calculations also suggest that the rate-determining step is the ring opening of the epoxide and is consistent with previous reports involving other metal-based catalysts.<sup>25,26,35</sup>

The second insertion has been computed starting from this weakly bonded dimer (Figure 3). For the sake of clarity, the discussion will be limited to the propagation step (no discussion about the chloride attack to lead to two equivalent propagating complexes will be done because aryloxides are, in general, better nucleophiles than chloride).

Coordination of the incoming second PO molecule occurs as expected at the cationic uranium center, leading to the disruption of the dimer. Thus, coordination is predicted to be endergonic by  $10.2$ – $18.6$  kcal·mol<sup>-1</sup>, which corresponds to the stabilization energy of the dimeric form reported earlier in this

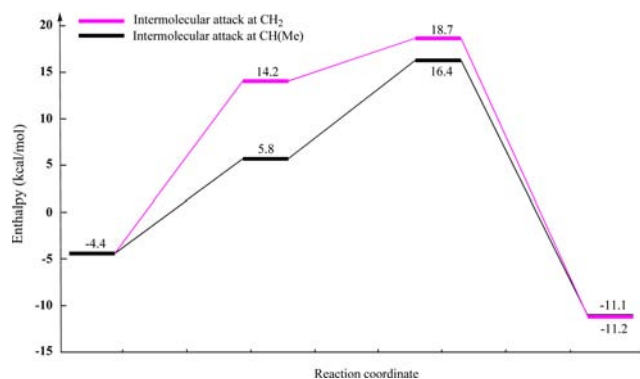


**Figure 3.** Enthalpy energy profile at 298.15 K for the second step of the reaction of PO with  $[\text{UO}_2\text{Cl}_2(\text{THF})_3]$ .

study. Coordination of the PO molecule is similar to that found in the first insertion reaction. This can be explained by the fact that the sterics (in particular, the bulkiness of the aryloxide group) mainly control coordination of the small PO molecule. In particular, the  $\text{U}-\text{O}$  distance is  $2.340$  Å and the  $\text{C}-\text{O}$  bond lengths are  $1.480$  and  $1.463$  Å. The TS is similar to the one found for the first insertion with an opened ring but with the  $\text{U}-\text{O}$  and  $\text{C}-\text{O}$  bonds not yet fully formed ( $2.245$  and  $2.238$  Å). The TS is thus still strongly ionic (charges: C,  $1.1157$ ; O,  $-1.5277$ ) explaining again the slight preference for the NA at the prochiral center (secondary carbon). Again, the difference of the barrier is within the error bar of the method, but this result is in excellent agreement with experimental data. The thermodynamics of the reaction is favorable in that case because it leads to the formation of two neutral species  $[\text{UO}_2\text{Cl}(\text{OCH}_2\text{CHMe})_2\text{Cl}(\text{THF})]$  and  $[\text{UO}_2\text{Cl}_2(\text{THF})]$ , which does not require dimerization. This step is thus exergonic by  $6.7$  kcal·mol<sup>-1</sup>.

On the basis of these findings, we have explored the reaction in more detail spectroscopically to confirm the dimeric nature of the propagating species. <sup>1</sup>H NMR spectroscopy proved to be

unhelpful because no specific resonances could be attributed to any propagating species. We therefore turned to fluorescence spectroscopy because this has proven to be a very sensitive technique and is useful in the determination of uranyl speciation in solution.<sup>36</sup> Low-temperature (77 K) fluorescence gives a spectrum dominated by “hot bands” that are slightly shifted in relation to  $[\text{UO}_2\text{Cl}_2(\text{THF})_3]$  (Figure 4). This

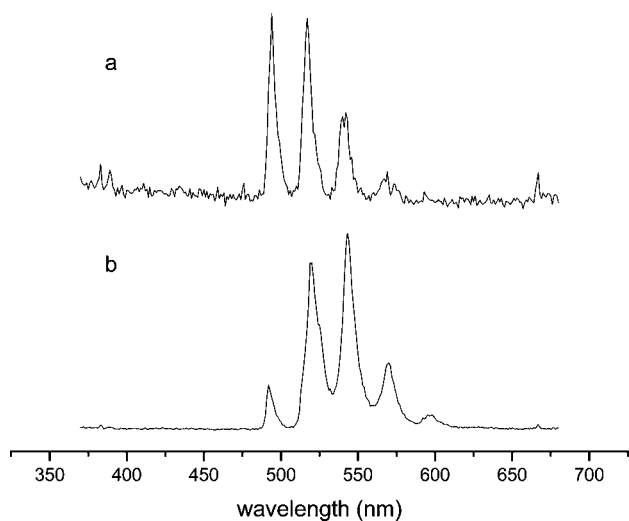


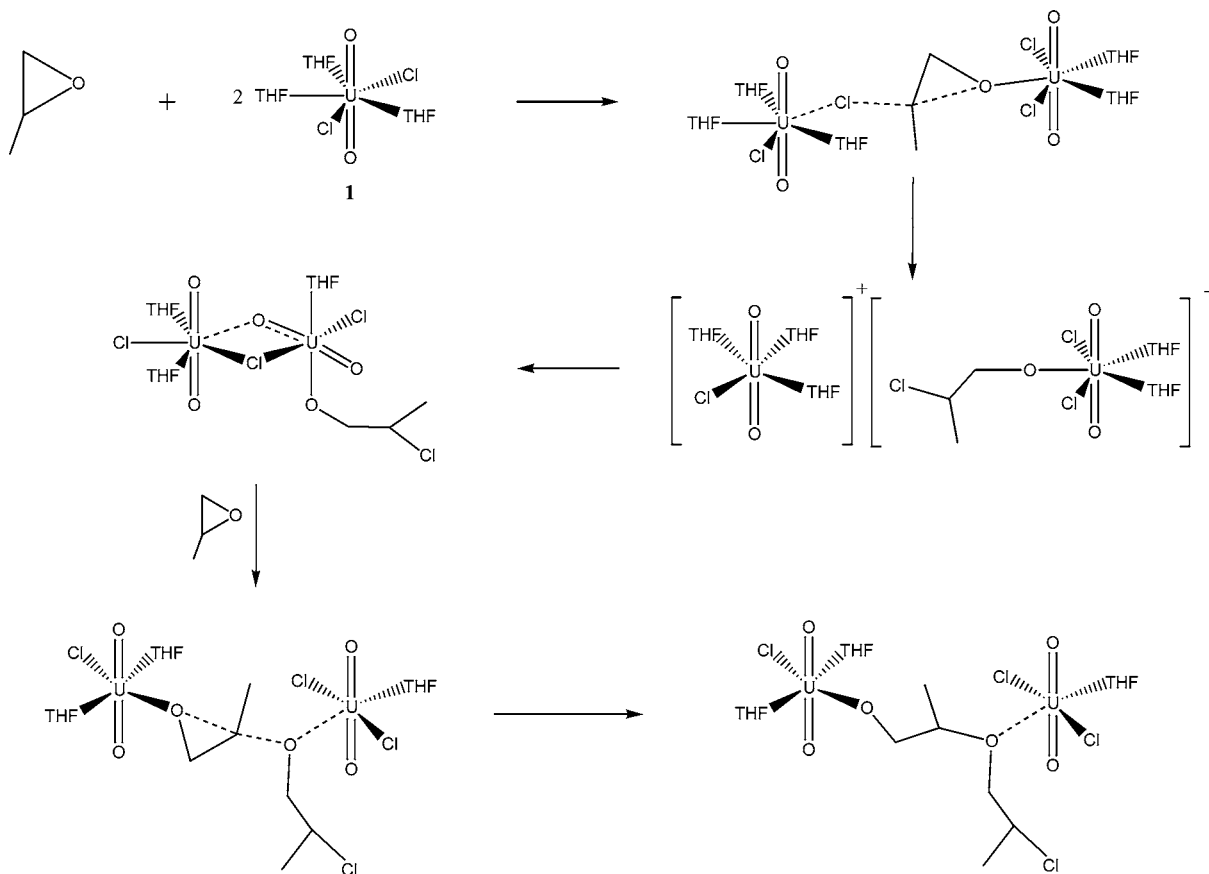
**Figure 4.** Emission spectrum of the reaction of  $[\text{UO}_2\text{Cl}_2(\text{THF})_3]$  (a) and  $[\text{UO}_2\text{Cl}_2(\text{THF})_3] + 10$  equiv of PO (b) in THF at 77 K ( $\lambda_{\text{ex}} = 350$  nm).

indicates that the dominant species in solution is electronically very similar to this, as predicted by the computations. The lifetime is very short at 7 ns, which is indicative of significant quenching, most likely due to exchange of THF and/or PO. This spectroscopic evidence suggests that the propagating species in solution is either monomeric or vibrationally isolated dimers. The latter is predicted computationally, but the former could be possible because the dimeric compound is weakly bound (roughly  $11.0 \text{ kcal}\cdot\text{mol}^{-1}$ ) and it could exchange with THF.

To summarize the results of the computational and experimental studies utilizing uranyl chloride as a catalyst, Scheme 4 illustrates the first two insertions of PO. In our original experimental report, we used *J*-resolved  $^1\text{H}$  NMR spectroscopy to examine the microstructure of the polymer formed from cyclohexene oxide, which gave strong evidence for an intermolecular mechanism involving two uranyl moieties. This has been confirmed as the most favorable for PO by the computations and has been traced to orbital control in the ring-opening TS. The mechanism for the uranyl aryloxide catalyst **2** has also been investigated theoretically and will be presented in the following section.

**Catalysis by Uranyl Aryloxide (2).** Unlike the uranyl chloride catalyst where a dimeric structure has been proven experimentally, only the pathways involving an inter- or intramolecular ring opening have been computed for the uranyl aryloxide catalyst **2** (Figure 5). The reaction begins by THF/PO exchange, which is computed to be accessible (between  $1.0$  and  $7.0 \text{ kcal}\cdot\text{mol}^{-1}$ ) and in line with the experimentally derived kinetic data. The main features of the

**Scheme 4. Computed Mechanism of the Ring-Opening Polymerization of PO Catalyzed by  $[\text{UO}_2\text{Cl}_2(\text{THF})_3]$**



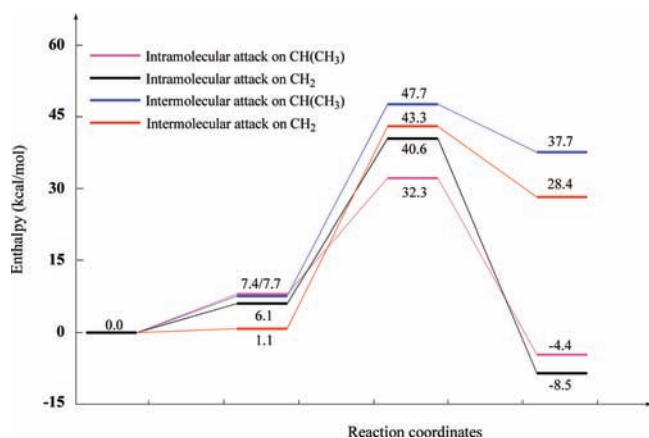


**Figure 5.** Enthalpy energy profile at 298.15 K for the first reaction of PO with the aryloxide catalyst.

PO coordination are similar to those reported for the chloride catalysts, and so these will not be discussed further. From this adduct, the NA TS is reached, and a clear difference between the considered pathways is observed. Indeed, the intermolecular pathway is found to be far less accessible than the intramolecular pathway. This is mainly ascribed to the steric effect due to the <sup>t</sup>Bu substituents on aryloxide that partially block the possible approach of a second uranyl aryloxide molecule. However, unlike the chloride, the bending of the aryl group allows a lone pair to point toward the empty orbital of the activated PO. The ring is almost already opened at the TS, where the carbocationic center now has a p orbital at an accessible geometry. Coupled to this, the U–O–C(ipsi) angle is 167° (compared to 180° in the reactant). Thus, due to these two effects, the first insertion will occur through an intramolecular route. This is the known pathway for the ring-opening polymerization of  $\epsilon$ -caprolactone, but there are little data on the initiation step for epoxide ring openings. Spectroscopic data on our system and other literature reports show that the propagation step is intermolecular.

As was already found for the chloride catalyst, the TS is highly ionic (C, 0.2989; O, -1.1091), explaining the kinetic preference for the attack at the prochiral center (Figure 5). It is noteworthy that the difference is clearly marked (difference of 8.3 kcal·mol<sup>-1</sup>). When the activation barriers for the reactions catalyzed by **1** and **2** are compared, it is interesting to note that, although aryloxide is better able to donate its electrons than chloride, its bulkiness induces an important steric repulsion that makes the aryloxide catalyst less efficient than the chloride catalyst for this first step. From a thermodynamic point of view, the reaction is exergonic. Interestingly, the product arising from the NA at the CH<sub>2</sub> center is found to be more stable than the CH, which is the kinetic product. This can account for the experimental observation of misinsertion in the polymer chain. Thus, in the second insertion, we have thus considered both the kinetic and thermodynamic products. In all cases, the four pathways considered in the first step were computed, leading to eight different pathways (Figure 6).

As for the chloride catalyst, only the propagation step has been considered here. Moreover, as was already stated earlier in this study, the reaction profile is very similar to that reported previously. The major difference is that the PO coordination is calculated to be an exergonic process by roughly 10.0 kcal·mol<sup>-1</sup>. For this second insertion, the intramolecular pathway is found to be kinetically less favorable than the

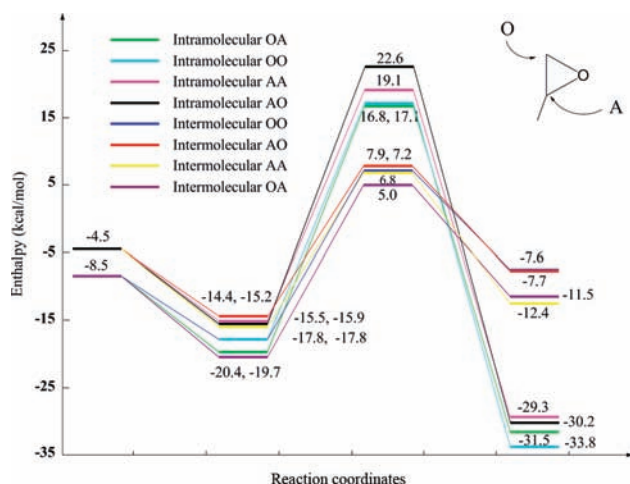


**Figure 6.** Enthalpy energy profile at 298.15 K for the second reaction of PO with the aryloxide catalyst.

intermolecular pathway by 11.0–15.0 kcal·mol<sup>-1</sup>. This can be attributed once again to steric effects. Indeed, the steric hindrance at the uranium center in the intramolecular pathway makes the second insertion less favorable than the first one. Thus, the intermolecular route becomes competitive and even more favorable than the intramolecular route. As in all previously described cases, the TS is strongly ionic, in line with the fact that the NA at the prochiral center is more favorable than that at the other carbon. Interestingly, starting from both products of the first insertion, this attack is the most favorable one. From the kinetic point of view, the reaction is found to be exergonic and is leading to the formation of an ion pair. However, unlike the chloride catalyst, the aryloxide ligand has a lower ability to adopt a bridging position. Moreover, the ion pair is found to be much less stable than the “neutral” intermolecular pair by roughly 15.0 kcal·mol<sup>-1</sup>, so that a rapid isomerization may occur. Thus, the propagation is also predicted to be intermolecular, as was already found for the chloride catalysts (Scheme 5).

On the basis of this theoretical finding, an experimental proof was looked for. Indeed, that the propagating species is dimeric is not unsurprising because steric bulk is the dominating factor in the degree of association of uranium coordination compounds. In particular, ligand redistribution reactions to form [U(OR)<sub>6</sub>] or aggregation into dimers, trimers, or tetramers can occur upon small changes to the ligand architecture.<sup>37</sup> In order to experimentally confirm that the propagating species is dimeric, we have used diffusion NMR spectroscopy because this is a straightforward method for determining the size of molecules in solution via calculation of the hydrodynamic radius,  $r_H$ , which has a reasonable correlation with the radii from crystallography.<sup>38</sup> The results of a diffusion NMR study of **2** and **2** + 10 equiv of PO in MeCN-*d*<sub>3</sub> are shown in Table 1. The results show that there is no significant change in the size of the molecules in solution, so as in the case for uranyl chloride, the major species in solution is monomeric.

In summary, we have elucidated the mechanism of the uranyl-catalyzed ring-opening polymerization of epoxides via a comprehensive computational study. In the case of the uranyl chloride catalyst, the initiation and propagation steps proceed via an intermolecular pathway, and this is driven by the inability of the lone pair on the chloride nucleophile to attack a PO molecule coordinated to the same metal center. Thus, the

Scheme 5. Schematic Representation of the Reaction Mechanism with Uranyl Aryloxide Catalyst

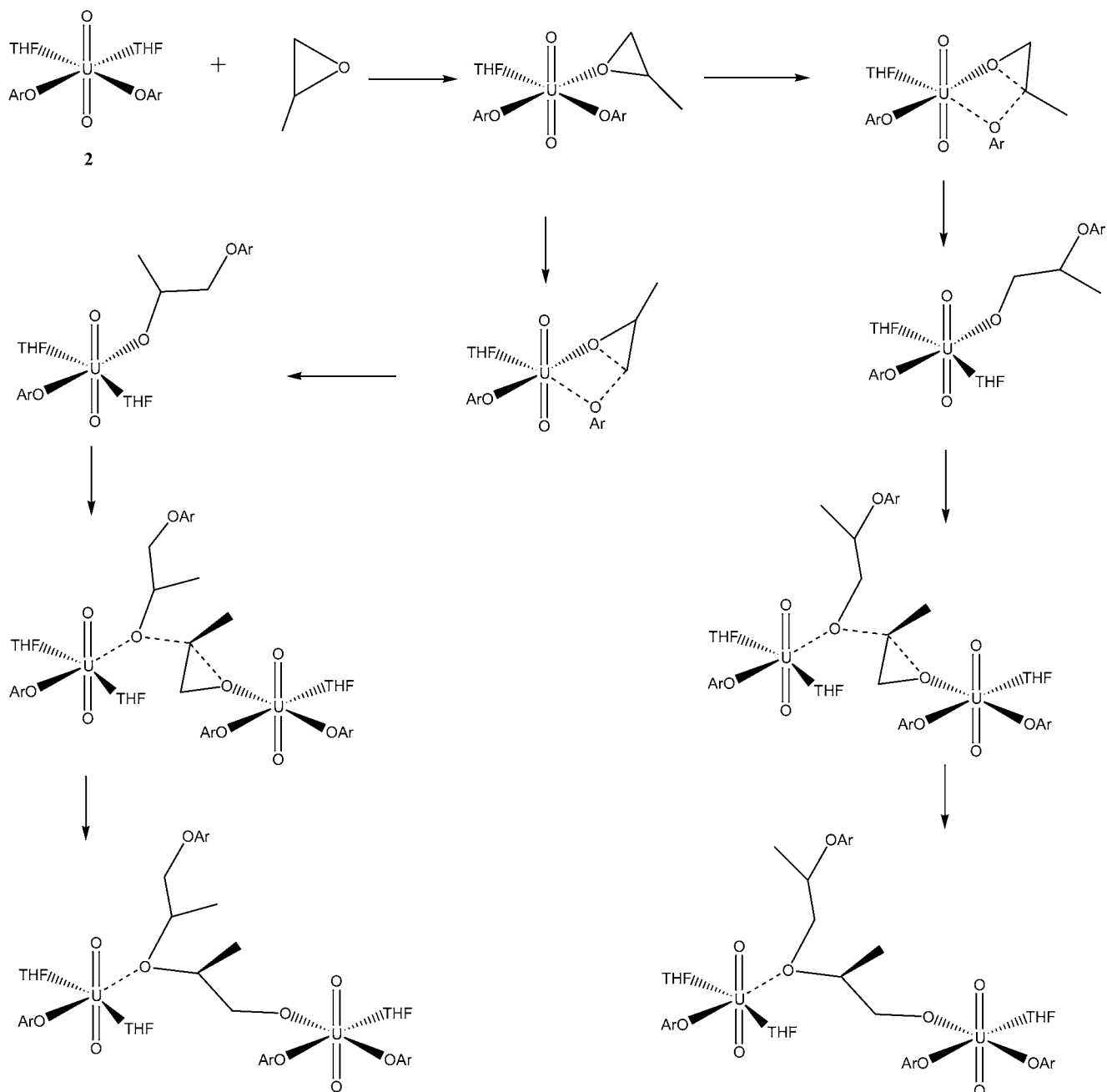


**Table 1. Diffusion Coefficient ( $D$ ) and Hydrodynamic Radius ( $r_H$ ) for 2 and 2 + PO at 0.1 M Concentrations in  $CD_3CN$  at 296 K**

compound	$D$ ( $\times 10^{-9} \text{ m}^2 \text{ s}^{-1}$ )	$r_H$ (Å)	$r_{X\text{-ray}}$ (Å)
2	$1.98 \pm 0.12$	4.82	$6.2^a$
2 + 10 equiv of PO	$1.76 \pm 0.09$	5.43	

<sup>a</sup>Deduced from the X-ray structure by considering the volume of the crystallographic cell divided by the number of molecules in the asymmetric unit.

initiation step is orbital-controlled. In contrast, the greater steric requirements of the bulkier aryloxide force the initiation step to be intramolecular, but propagation goes via an intermolecular pathway. This computational study explains a number of the experimental features. The computations on the mechanism are

some of the largest carried out for any uranium-based study in the literature and suggest that, despite the inherent difficulties in actinide computational chemistry, DFT is a powerful technique for studying catalysis featuring uranium atoms.

## ■ ASSOCIATED CONTENT

### Supporting Information

Full details of the computations, NMR, and fluorescence measurements. This material is available free of charge via the Internet at <http://pubs.acs.org>.

## ■ AUTHOR INFORMATION

### Corresponding Author

\*E-mail: bakerrj@tcd.ie (R.J.B.), laurent.maron@irsamc.upstlse.fr (L.M.).

## Notes

The authors declare no competing financial interest.

## ACKNOWLEDGMENTS

We thank IRCSET for funding this work through the EMBARK initiative, and the French Ministry of Research and Higher Education, INSA, and UPS are thanked for financial support. L.M. is grateful to the Institut Universitaire de France. CalMip (CNRS, Toulouse, France) and CINES (CNRS, Montpellier, France) are acknowledged for calculation facilities. J.F. is thankful for financial support from the Chinese Scholarship Council and the Scholarship Council of Lanzhou University.

## REFERENCES

- (1) (a) Hayton, T. W. *Dalton Trans.* **2010**, *39*, 1145–1158. (b) Liddle, S. T.; Mills, D. P. *Dalton Trans.* **2009**, 5592–5605. (c) Lam, O. P.; Anthon, C.; Meyer, K. *Dalton Trans.* **2009**, 9677–9691. (d) Graves, C. R.; Kiplinger, J. L. *Chem. Commun.* **2009**, 3831–3853. (e) Liddle, S. T. *Proc. R. Soc. London A* **2009**, *465*, 1673–1700. (f) Castro-Rodríguez, I.; Meyer, K. *Chem. Commun.* **2006**, 1353–1368. (g) Ephritikhine, M. *Dalton Trans.* **2006**, 2501–2516.
- (2) (a) Lam, O. P.; Meyer, K. *Polyhedron* **2012**, *32*, 1–9. (b) Arnold, P. L. *Chem. Commun.* **2011**, *47*, 9005–9010. (c) Summerscales, O. T.; Cloke, F. G. N. *Struct. Bonding (Berlin)* **2008**, *127*, 87–117.
- (3) For recent reviews, see: (a) Weiss, C. J.; Marks, T. J. *Dalton Trans.* **2010**, *39*, 6576–6588. (b) Eisen, M. S. *Top. Organomet. Chem.* **2010**, *31*, 157–184. (c) Fox, A. R.; Bart, S. C.; Meyer, K.; Cummins, C. C. *Nature* **2008**, *455*, 341–349. (d) Andrea, T.; Eisen, M. S. *Chem. Soc. Rev.* **2008**, *37*, 550–567. (e) Barnea, E.; Eisen, M. S. *Coord. Chem. Rev.* **2006**, *250*, 855–899. (f) Burns, C. J.; Eisen, M. S. In *The Chemistry of the Actinide and Transactinide Elements*; Morss, L. R., Edelstein, N., Fuger, J., Eds.; Springer: Dordrecht, The Netherlands, 2006; Vol. 5, pp 2911–3012.
- (4) Broderick, E. M.; Gutzwiller, N. P.; Diaconescu, P. L. *Organometallics* **2010**, *29*, 3242–3251.
- (5) Lin, Z.; Marks, T. J. *J. Am. Chem. Soc.* **1987**, *109*, 7979–7985.
- (6) (a) Rabinovich, E.; Aharonovich, S.; Botoshansky, M.; Eisen, M. S. *Dalton Trans.* **2010**, *39*, 6667–6676. (b) Barnea, E.; Moradove, D.; Berthet, J.-C.; Ephritikhine, M.; Eisen, M. S. *Organometallics* **2006**, *25*, 320–322.
- (7) (a) Sharma, M.; Andrea, T.; Brookes, N. J.; Yates, B. F.; Eisen, M. S. *J. Am. Chem. Soc.* **2011**, *133*, 1341–131356. (b) Andrea, T.; Banea, E.; Eisen, M. S. *J. Am. Chem. Soc.* **2008**, *130*, 2454–2455.
- (8) Peters, R. G.; Warner, B. P.; Burns, C. J. *J. Am. Chem. Soc.* **1999**, *121*, 5585–5586.
- (9) For uranium(VI) compounds in catalysis, see: (a) van Axel Castelli, V.; Dalla Cort, A.; Mandolini, L.; Reinhoudt, D. N.; Schiaffino, L. *Eur. J. Org. Chem.* **2003**, 627–633 and references cited therein. (b) Moss, R. A.; Bracken, K.; Zhang, J. *Chem. Commun.* **1997**, 563–564. (c) Enthaler, S. *Chem.—Eur. J.* **2011**, *17*, 9316–9319.
- (10) Baker, R. J.; Walshe, A. *Chem. Commun.* **2012**, *48*, 985–987.
- (11) The bond disruption energy of a U<sup>IV</sup>–O bond is 307 ± 13 kJ·mol<sup>-1</sup>. Leala, J. P.; Marques, N.; Takats, J. J. *Organomet. Chem.* **2001**, *632*, 209–214.
- (12) The release of ring strain has been implicated in CO<sub>2</sub>/epoxide copolymerizations. See: Liu, Z.; Torrent, M.; Morokuma, K. *Organometallics* **2002**, *21*, 1056–1071.
- (13) Wilkerson, M. P.; Burns, C. J.; Morris, D. E.; Paine, R. T.; Scott, B. L. *Inorg. Chem.* **2002**, *41*, 3110.
- (14) For recent reviews, see: (a) Dolg, M.; Cao, X. In *Encyclopedia of Inorganic Chemistry*, 2nd ed.; John Wiley & Sons, Ltd.: New York, 2006. (b) Gagliardi, L.; Roos, B. O. *Chem. Soc. Rev.* **2007**, *36*, 893–903. (c) Kaltsoyannis, N. *Chem. Soc. Rev.* **2003**, *32*, 9–16.
- (15) Kaltsoyannis, N.; Hay, P. J.; Li, J.; Blaudeau, J.-P.; Bursten, B. E. In *The Chemistry of the Actinide and Transactinide Elements*; Morss, L. R., Edelstein, N., Fuger, J., Eds.; Springer: Dordrecht, The Netherlands, 2006; Vol. 3, pp 1893–2012.
- (16) Wilkerson, M. P.; Burns, C. J.; Paine, R. T.; Scott, B. L. *Inorg. Chem.* **1999**, *38*, 4156–4158.
- (17) Frisch, M. J.; Trucks, G. W.; Schlegel, H. B.; Scuseria, G. E.; Robb, M. A.; Cheeseman, J. R.; Scalmani, G.; Barone, V.; Mennucci, B.; Petersson, G. A.; Nakatsuji, H.; Caricato, M.; Li, X.; Hratchian, H. P.; Izmaylov, A. F.; Bloino, J.; Zheng, G.; Sonnenberg, J. L.; Hada, M.; Ehara, M.; Toyota, K.; Fukuda, R.; Hasegawa, J.; Ishida, M.; Nakajima, T.; Honda, Y.; Kitao, O.; Nakai, H.; Vreven, T.; Montgomery, J. A., Jr.; Peralta, J. E.; Ogliaro, F.; Bearpark, M.; Heyd, J. J.; Brothers, E.; Kudin, K. N.; Staroverov, V. N.; Kobayashi, R.; Normand, J.; Raghavachari, K.; Rendell, A.; Burant, J. C.; Iyengar, S. S.; Tomasi, J.; Cossi, M.; Rega, N.; Millam, J. M.; Klene, M.; Knox, J. E.; Cross, J. B.; Bakken, V.; Adamo, C.; Jaramillo, J.; Gomperts, R.; Stratmann, R. E.; Yazyev, O.; Austin, A. J.; Cammi, R.; Pomelli, C.; Ochterski, J. W.; Martin, R. L.; Morokuma, K.; Zakrzewski, V. G.; Voth, G. A.; Salvador, P.; Dannenberg, J. J.; Dapprich, S.; Daniels, A. D.; Farkas, O.; Foresman, J. B.; Ortiz, J. V.; Cioslowski, J.; Fox, D. J. *Gaussian09*, revision A.02; Gaussian, Inc.: Wallingford, CT, 2009.
- (18) Becke, A. D. *J. Chem. Phys.* **1993**, *98*, 5648–5652.
- (19) Perdew, J. P.; Wang, Y. *Phys. Rev. B* **1992**, *45*, 13244–13249.
- (20) Moritz, A.; Cao, X. Y.; Dolg, M. *Theor. Chem. Acc.* **2007**, *118*, 845–854.
- (21) (a) Castro, L.; Yahia, A.; Maron, L. *ChemPhysChem* **2010**, *11*, 990–994. (b) Castro, L.; Yahia, A.; Maron, L. *Dalton Trans.* **2010**, *39*, 6682–6692.
- (22) (a) Ditchfield, R.; Hehre, W. J.; Pople, J. A. *J. Chem. Phys.* **1971**, *54*, 724–728. (b) Hehre, W. J.; Ditchfield, R.; Pople, J. A. *J. Chem. Phys.* **1972**, *56*, 2257–2261. (c) Hariharan, P. C.; Pople, J. A. *Theor. Chim. Acta* **1973**, *28*, 213–223.
- (23) Schlegel, H. B. *J. Comput. Chem.* **1982**, *3*, 214–218.
- (24) (a) Gonzalez, C.; Schlegel, H. B. *J. Chem. Phys.* **1989**, *90*, 2154–2161. (b) Gonzalez, C.; Schlegel, H. B. *J. Phys. Chem.* **1990**, *94*, 5523–5527.
- (25) For selected examples, see: (a) Schön, E.; Zhang, X.; Zhou, Z.; Chisholm, M. H.; Chen, P. *Inorg. Chem.* **2004**, *43*, 7278–7280. (b) Antelmann, B.; Chisholm, M. H.; Iyer, S. S.; Huffman, J. C.; Navarro-Llobet, D.; Pagel, M.; Simonsick, W. J.; Zhong, W. *Macromolecules* **2001**, *34*, 3159–3175. (c) Braune, W.; Okuda, J. *Angew. Chem., Int. Ed.* **2003**, *42*, 64–67. (d) Chisholm, M. H.; Crandall, J. K.; McCollum, D. G.; Pagel, M. *Macromolecules* **1999**, *32*, 5744–5746. (e) Ajiro, H.; Allen, S. D.; Coates, G. W. In *Stereoselective Polymerization with Single-Site Catalysts*; Baugh, L. S., Canich, J. M., Eds.; CRC Press: Boca Raton, FL, 2007; p 627.
- (26) For recent reviews, see: (a) Klaus, S.; Lehenmeier, M. W.; Anderson, C. E.; Rieger, B. *Coord. Chem. Rev.* **2011**, *25*, 1460–1479. (b) Darensbourg, D. J. *Chem. Rev.* **2007**, *107*, 2388–2410. (c) Kember, M. R.; Buchard, A.; Williams, C. K. *Chem. Commun.* **2011**, *47*, 141–163. (d) Coates, G. W.; Moore, D. R. *Angew. Chem., Int. Ed.* **2004**, *43*, 6618–6639.
- (27) Jacobsen, E. N. *Acc. Chem. Res.* **2000**, *33*, 421–431.
- (28) Hirahata, W.; Thomas, R. M.; Lobkovsky, E. B.; Coates, G. W. *J. Am. Chem. Soc.* **2008**, *130*, 17658–17659. (b) Widger, P. C. B.; Ahmed, S. M.; Hirahata, W.; Thomas, R. M.; Lobkovsky, E. B.; Coates, G. W. *Chem. Commun.* **2010**, *46*, 2935–2937.
- (29) (a) Mukhopadhyay, A.; Pandey, P.; Chakraborty, T. *J. Phys. Chem. A* **2010**, *114*, 5026–5033. (b) Aue, D. H.; Webb, H. M.; Davidson, W. R.; Vidal, M.; Bowers, M. T.; Goldwhite, H.; Vertal, L. E.; Douglas, J. E.; Kollman, P. A.; Kenyon, G. L. *J. Am. Chem. Soc.* **1980**, *102*, 5151–5157. (c) West, R.; Powell, D. L.; Lee, M. K. T.; Whatley, L. S. *J. Am. Chem. Soc.* **1964**, *86*, 3227–3229.
- (30) Fortier, S.; Hayton, T. W. *Coord. Chem. Rev.* **2010**, *254*, 197–214.
- (31) For example, see: (a) Mihalcea, I.; Henry, N.; Clavier, N.; Dacheux, N.; Loiseau, T. *Inorg. Chem.* **2011**, *50*, 6243–6249. (b) Sullens, T. A.; Jensen, R. A.; Shvareva, T. Y.; Albrecht-Schmitt, T. E. *J. Am. Chem. Soc.* **2004**, *126*, 2676–2677.
- (32) Darensbourg, D. J.; Billodeaux, D. R.; Perez, L. M. *Organometallics* **2004**, *23*, 5286–5290.



(33) Darensbourg, D. J.; Niezgod, S. A.; Draper, J. D.; Reibenspies, J. H. *J. Am. Chem. Soc.* **1998**, *120*, 4690–4698.

(34) Darensbourg, D. J.; Wildeson, J. R.; Lewis, S. J.; Yarbrough, J. C. *J. Am. Chem. Soc.* **2002**, *124*, 7075–7083.

(35) Klaus, S.; Vagin, S. I.; Lehenmeier, M. W.; Deglmann, P.; Brym, A. K.; Rieger, B. *Macromolecules* **2011**, *44*, 9508–9516.

(36) (a) Natrajan, L. S. *Coord. Chem. Rev.* **2012**, *256*, 1583–1563.

(b) Redmond, M. P.; Cornet, S. M.; Woodall, S. D.; Whittaker, D.; Collison, D.; Helliwell, M.; Natrajan, L. S. *Dalton Trans.* **2011**, *40*, 3914–3926.

(37) Wilkerson, M. P.; Burns, C. J.; Dewey, H. J.; Martin, J. M.; Morris, D. E.; Paine, R. T.; Scott, B. L. *Inorg. Chem.* **2000**, *39*, 5277–5285. Burns, C. J.; Sattelberger, A. P. *Inorg. Chem.* **1988**, *27*, 3692–3693.

(38) For selected reviews, see: (a) Macchioni, A.; Ciancaleoni, G.; Zuccaccia, C.; Zuccaccia, D. *Chem. Soc. Rev.* **2008**, *37*, 479–489.

(b) Pregosin, P. S.; Kumar, P. G. A.; Fernández, I. *Chem. Rev.* **2005**, *105*, 2977–2998.